

# ClearDepth: Enhanced Stereo Perception of Transparent Objects for Robotic Manipulation

Kaixin Bai<sup>1,2</sup>, Huajian Zeng<sup>2,3</sup>, Lei Zhang<sup>1,2†</sup>, Yiwen Liu<sup>2,3</sup>, Hongli Xu<sup>3</sup>, Zhaopeng Chen<sup>2</sup>, Jianwei Zhang<sup>1</sup>

**Abstract**—Transparent object depth perception poses a challenge in everyday life and logistics, primarily due to the inability of standard 3D sensors to accurately capture depth on transparent or reflective surfaces. This limitation significantly affects depth map and point cloud-reliant applications, especially in robotic manipulation. We developed a vision transformer-based algorithm for stereo depth recovery of transparent objects. This approach is complemented by an innovative feature post-fusion module, which enhances the accuracy of depth recovery by structural features in images. To address the high costs associated with dataset collection for stereo camera-based perception of transparent objects, our method incorporates a parameter-aligned, domain-adaptive, and physically realistic Sim2Real simulation for efficient data generation, accelerated by AI algorithm. Our experimental results demonstrate the model’s exceptional Sim2Real generalizability in real-world scenarios, enabling precise depth mapping of transparent objects to assist in robotic manipulation. Project details are available at <https://sites.google.com/view/cleardepth/>.

## I. INTRODUCTION

Transparent objects, such as glass bottles or cups, are commonly found in domestic service robotics and logistics goods sorting scenarios. Their transparent nature, particularly the complexity of refraction and reflection, poses challenges for imaging and recognition [1]. Accurate handling of these objects is crucial for robots that rely on precise three-dimensional information. Whether it’s accurately grasping glass items in home services or efficiently sorting transparent goods at logistics centers, advanced algorithms and technologies are required for machine vision systems. This includes the development of algorithms capable of handling materials with high reflectivity and refraction, or new sensor technologies to better capture the characteristics of transparent objects. These advancements will enhance the ability of robots to handle transparent objects in various environments, push the application of robotic vision technology into broader fields, and enable robots to perform complex tasks more autonomously. In addressing the depth perception challenges posed by transparent objects, researchers have developed innovative approaches. Initial efforts focused on using deep learning techniques to reconstruct depth information from incomplete depth images captured by RealSense cameras, optimizing for greater accuracy [2], [3]. Subsequent studies explored stereo vision systems [4] and multi-view approaches [5], leveraging neural networks to enhance perception capabilities. Despite these advancements, real-world applications still face challenges, such as inconsistent depth inputs and the complexities of multi-view imaging. A major

obstacle in 3D reconstruction of transparent objects is the scarcity of reliable feature points. Innovations addressing this include extracting structural details, such as boundary identification [6], and improving hardware capabilities for more accurate depth imagery [7]. Deep learning has played a pivotal role in learning and interpreting the complex geometric features of these objects, thereby enhancing the precision and reliability of 3D models. For deep learning tasks involving transparent objects, extensive and accurate datasets are crucial. Various techniques have been used for dataset collection, including using markers for object poses [8], [9], substituting transparent objects with opaque ones [10], and manual manipulation in 3D software [11]. However, these methods are labor-intensive and often result in noisy depth maps. To overcome these challenges, simulation engines are increasingly used to generate synthetic data [11], [5], though balancing the realism of ray-tracing with the efficiency of rasterization remains a significant challenge. Our approach includes developing an AI-accelerated tool for generating realistic simulation datasets for transparent object depth recovery. This tool enables direct application of models on actual sensors without post-training, producing instance segmentation, poses, and depth maps. We also introduce a stereo depth recovery network specifically designed for transparent objects. Utilizing a cascaded vision transformer (ViT) backbone, it efficiently extracts contextual structural information. This network outperforms previous CNN and ViT-based models, particularly for high-resolution images and robotic manipulation. Our contributions address the limitations of existing depth estimation methods and datasets for transparent objects. We present a novel AI-enhanced stereo-based simulation dataset generation method, creating a detailed, noise-free dataset. Additionally, our end-to-end stereo depth recovery network operates independently of mask priors and includes a post-processing structure that enhances structural details. This stereo imaging algorithm can be directly integrated into existing robotic grasping pipelines. The whole pipeline is as in Fig. 1.

## II. RELATED WORK

### A. Perception of Transparent Objects

Robotics faces significant challenges in perceiving transparent objects due to their low contrast and complex light behavior, which affects sensor accuracy in determining their position and shape. Traditional sensors like RGB and RGB-D cameras often struggle with transparent objects because they focus on intensity data, missing the nuances of optical properties. To address this, research has increasingly turned to polarized cameras, which reduce reflections, increase contrast, and provide richer light information, enhancing the detection of transparent objects’ shape and position [7],

†Corresponding author. lei.zhang-1@studium.uni-hamburg.de

<sup>1</sup>MIN-Fakultät Fachbereich Informatik TAMS, University of Hamburg {name.surname}@studium.uni-hamburg.de

<sup>2</sup>Agile Robots SE {name.surname}@agile-robots.com

<sup>3</sup>Technical University of Munich {name.surname}@tum.de

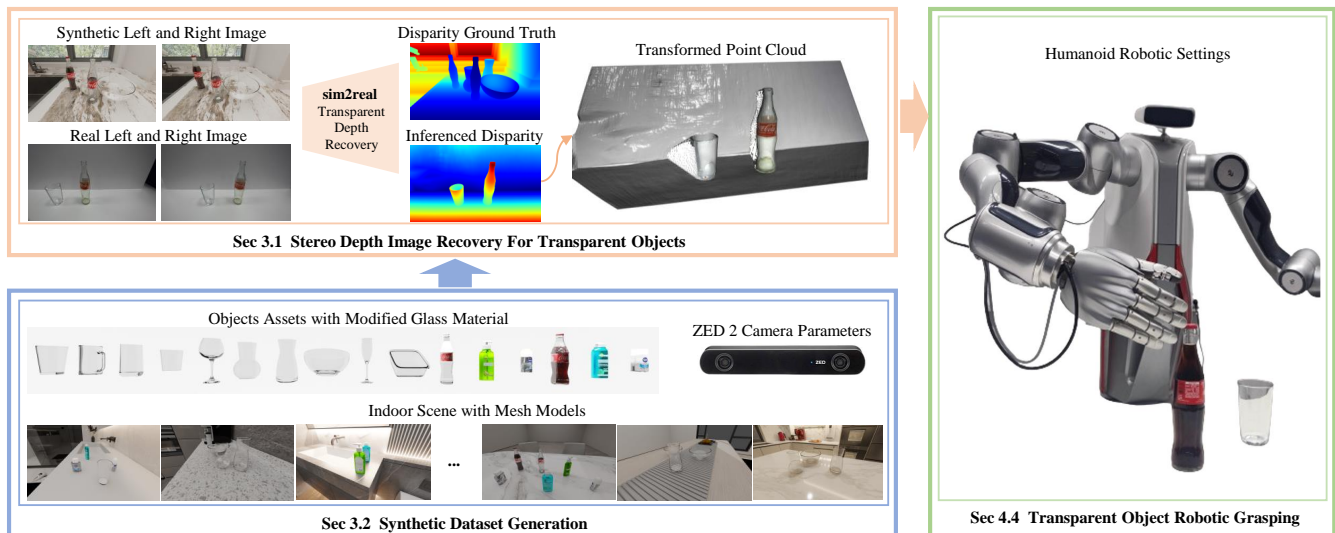


Fig. 1: In this work, we explore how to reconstruct depth maps of transparent objects using Sim2Real technology combined with stereo vision, thereby enabling precise manipulation of transparent objects by robots. In the Section III, we focus on introducing a simulation data generation method enhanced by AI, aimed at achieving an optimal balance between the effectiveness and speed of data generation. The Section IV conducts both qualitative and quantitative analyses comparing the performance of our method with the baseline, and demonstrates the efficacy of our approach through robot grasping experiments.

[12]. However, their high cost limits widespread use in robotics. Some studies, like [13], enhance transparent object tracking by combining CNN and transformer-based encoders, while [14] employs Sim2Real strategies with simulated datasets. Research such as [15] addresses transparent object matting by predicting alpha channel values, aiding image editing. For robotic manipulation and pose estimation, recent works have expanded perception models to include multi-task extensions [8], [11], [16]. Depth recovery and reconstruction remain particularly challenging due to light interactions, with techniques like Nerf and volumetric rendering used for surface reconstruction [17], [7], [18], [19], and stereo and multiview approaches for depth and geometry regression [4], [20], [9]. These efforts utilize various sensors, including RGB-D, stereo-vision, and multi-view systems, to improve transparent object perception [3], [2], [8], [11], [16], [9], [4], [5], [18], [7]. The field, while complex, is advancing with deep learning and sensor technology, aiming to enhance accuracy and reliability.

### B. Deep Learning-based Stereo Depth Recovery

Deep learning-based stereo matching methods have recently outperformed traditional approaches, with 2D convolutional models [21], [22] offering simplicity and efficiency. These models achieve high accuracy even on limited computational resources, making them suitable for engineering applications, though they still require improvements in accuracy and robustness due to 3D cost space constraints. 3D convolutional networks [23], [24] provide better interpretability and higher disparity map accuracy but require optimization due to their computational demands. RAFT-Stereo [25], an extension of RAFT [26], applies optical flow techniques to stereo matching, improving generalization and robustness with its lightweight GRU module, but struggles with global context extraction due to its CNN architecture. STTR [27],

inspired by SuperGlue [28], uses transformers with positional embedding and attention mechanisms for binocular dense matching, producing disparity and depth maps. However, these methods are computationally intensive and slow in inference, limiting their suitability for high-resolution images and downstream robotic tasks.

### C. Transparent Object Datasets

In the open-source community, various datasets for transparent objects are available, such as real-world datasets [8], [29], [30]. In Depth Anything v1, the authors used both open-source real and synthetic datasets for training, but in v2, they switched entirely to synthetic data. Introducing even 10% real data can significantly degrade performance due to sensor noise in the labels, which is particularly detrimental in depth recovery tasks. The challenge of accurately annotating complex, occluded real-world scenes led us to prioritize synthetic data. To mitigate potential sim2real gaps, we used ray-tracing renderers to simulate realistic light refraction. Existing synthetic datasets, such as [10], [31], [9], [32], [33], [16], typically feature transparent objects on desktops. However, these datasets lack the complexity necessary for generalization to real-world scenarios like kitchens, bedrooms, and offices, where service and humanoid robots operate. Moreover, these datasets often require extensive pre- or post-processing, such as segmentation or background reconstruction, which is impractical for end-to-end algorithms crucial to embodied intelligence applications. Synthetic datasets with HDRI backgrounds, such as [5], also face challenges. HDRI backgrounds lack depth value labels, leading to confusion and poor generalization, especially in zero-shot scenarios for service robots. Simulation data for RealSense cameras, like [16], [33], involve complex rendering processes that reduce efficiency. The process includes rendering the RGB image, simulating IR projection with

spotlights, and generating noisy depth maps, which is both complex and time-consuming. In designing our dataset and generation process, we address the limitations of existing datasets while anticipating the needs of future embodied intelligence algorithms. Our dataset includes indoor scenes typical for service robots, enriched with background depth values for transparent objects. It features both container-type and cosmetic transparent objects, carefully designed to overcome current deficiencies and ensure future scalability.

### III. METHOD

#### A. Network Overview

Transparent objects refract background textures, making texture features less relevant and structural features more critical for imaging and perception tasks. In [34], it was found that CNNs excel at recognizing textures, while ViTs are better at recognizing shapes. Traditional ViTs downsample inputs and outputs to a smaller size, using learnable upsampling. While effective in many vision tasks, ViTs are challenging to train, computationally intensive, and less effective at fine-grained feature extraction. To address this, models like SegFormer [35] and DinoV2 [36] use cascaded structures to enhance ViTs for fine-grained tasks like depth estimation and semantic segmentation, providing multi-scale features and easing training.

For transparent objects, structural features are crucial. Considering the fine-grained needs of stereo tasks and the demand for lightweight, fast models in robotics, we utilize MixVisionTransformer B5 for feature extraction. Traditional stereo deep learning networks rely on feature dot products for similarity, which is inadequate for transparent objects due to background texture refraction. Incorporating structural feature priors in the GRU loop is essential. While cross-attention or spatial-attention structures could be used, they are parameter-heavy and slow in inference. Therefore, we designed a lightweight structural feature post-fusion module to introduce these features into the GRU loop, enhancing performance by leveraging the low-level structural feature. Our network structure is as in Fig. 2.

1) *Cascaded Vision Transformer Backbone.*: Our backbone architecture, conforming to the B5 settings of SegFormer, initiates with overlap patch embedding for initial image tokenization, crucial for preserving local features. This process sequentially passes the tokens through four transformer blocks ( $N = 4$ ), effectively generating feature maps at scaled dimensions of  $\frac{1}{4}$ ,  $\frac{1}{8}$ ,  $\frac{1}{16}$ , and  $\frac{1}{32}$ . To optimize computational efficiency, the model incorporates efficient self-attention, which significantly reduces the computational burden from  $O(N^2)$  to  $O(\frac{N^2}{R})$  by implementing a reduction ratio  $R$ . This reduction is achieved by first reshaping the input sequence from  $N \cdot C$  to  $\frac{N}{R} \times (C \cdot R)$  by 2d convolutional layer with the stride 8, 4, 2, 1 for different ViT blocks, as detailed in equation 1, and then adjusting the sequence dimensions back to  $C$  through linear layers, as described in equation 2.

$$\hat{K} = \text{Reshape}(\frac{N}{R}, C \cdot R)(K) \quad (1)$$

$$K = \text{Linear}(C \cdot R, C)(\hat{K}) \quad (2)$$

Additionally, the Mix-FFN module in the architecture addresses the challenge of performance degradation due to

the interpolation of positional embeddings in the original ViT structure, especially when dealing with varying input image sizes, here by substituting positional embeddings with learnable depth-wise convolutions. The equation is as 3.

$$\mathbf{x}_{\text{out}} = \text{MLP}(\text{GELU}(\text{Conv}_{3 \times 3}(\text{MLP}(\mathbf{x}_{\text{in}})))) + \mathbf{x}_{\text{in}} \quad (3)$$

Then, we concatenate multi-scale feature maps from different ViT blocks by upsampling them to a unified scale of  $\frac{1}{4}$ . This combined feature map undergoes further refinement through a precise  $1 \cdot 1$  convolution, facilitating optimal dimension adjustment.

2) *Structural Feature Post-Fusion*: In this work, we propose a modified GRU-based architecture to optimize disparity maps in a coarse-to-fine manner. Our Post-Fusion modification is particularly introduced to enhance the processing of transparent objects. We made this modification because, during our depth estimation experiments on transparent objects, we observed that unlike regular objects, depth estimation for transparent objects particularly requires precise structural information. Additionally, for transparent objects, due to the refractive nature of their background texture features, the feature similarity information obtained through dot product is not suitable for reconstructing transparent objects. Therefore, it makes sense to introduce the structural information of the image itself during the GRU iterations. This approach ensures that the structural information extracted at different resolutions remains consistent throughout the iterative process.

The core update equations in our model are defined as follows:

$$x_k = [\mathbf{C}_k, \mathbf{d}_k, \mathbf{c}_k, \mathbf{c}_r, \mathbf{c}_h] \quad (4)$$

$$z_k = \sigma(\text{Conv}([h_{k-1}, x_k], W_z) + c_k), \quad (5)$$

$$r_k = \sigma(\text{Conv}([h_{k-1}, x_k], W_r) + c_r), \quad (6)$$

$$\tilde{h}_k = \tanh(\text{Conv}([r_k \odot h_{k-1}, x_k], W_h) + c_h), \quad (7)$$

$$h_k = (1 - z_k) \odot h_{k-1} + z_k \odot \tilde{h}_k, \quad (8)$$

Here,  $x_k$  is a concatenation of several feature maps, including the correlation  $\mathbf{C}_k$ , the current disparity  $\mathbf{d}_k$ , and structural context features  $\mathbf{c}_k$ ,  $\mathbf{c}_r$ , and  $\mathbf{c}_h$ . Specifically,  $\mathbf{c}_k$ ,  $\mathbf{c}_r$ , and  $\mathbf{c}_h$  represent structural features derived from the left image. These features are incorporated as residuals into the GRU loop, allowing for enhanced participation of structural information during the disparity map refinement process.

Then, Our approach decode GRUs at each resolutions to obtain multi-scale disparity updates for coarse to fine gradual optimization:

$$\Delta \mathbf{d}_{k, \frac{1}{32}} = \text{Decoder}(h_{k, \frac{1}{32}}), \quad (9)$$

$$\Delta \mathbf{d}_{k, \frac{1}{16}} = \text{Decoder}(h_{k, \frac{1}{16}} + \text{Interp}(\Delta \mathbf{d}_{k, \frac{1}{32}})), \quad (10)$$

$$\Delta \mathbf{d}_{k, \frac{1}{8}} = \text{Decoder}(h_{k, \frac{1}{8}} + \text{Interp}(\Delta \mathbf{d}_{k, \frac{1}{16}})), \quad (11)$$

where Decoder consist of two convolutional layers and Interp is bilinear interpolation scaled up by a factor of two. Finally, the updated disparity is calculated as:

$$\mathbf{d}_{k+1} = \mathbf{d}_k + \Delta \mathbf{d}_k \quad (12)$$

In summary, to address the challenges of transparent objects, we selected an appropriate image feature extractor.

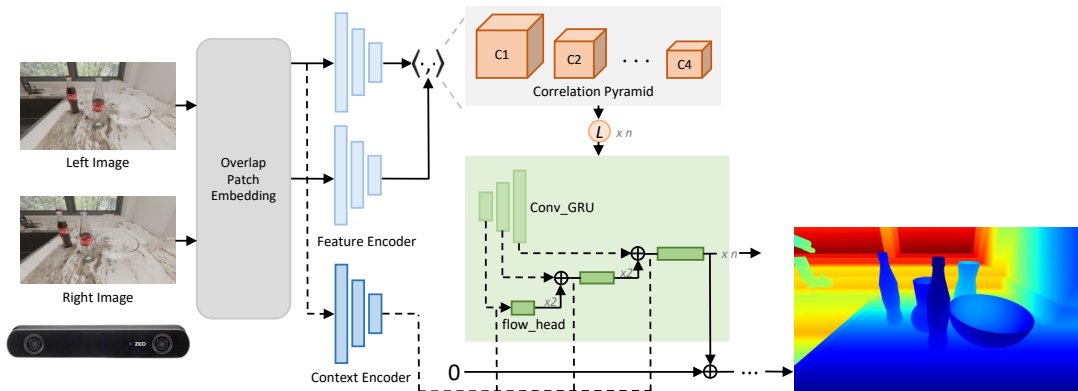


Fig. 2: Our stereo depth recovery network for transparent objects. Feature extraction is performed on left and right images, with additional processing by a shared weighted context encoder for the left image. A correlation pyramid, created by merging the feature maps, is refined through a GRU loop, enhancing structural information for depth recovery. The output is a refined disparity map.

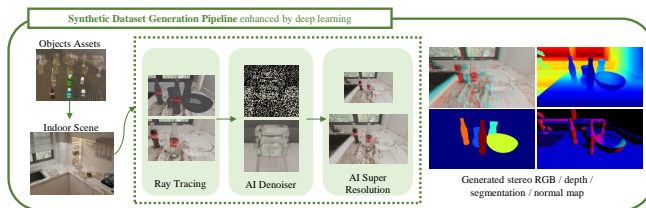


Fig. 3: We utilize hardware-accelerated ray tracing, OptiX AI denoiser, and AI-driven super-resolution. This process accelerates the dataset generation process.

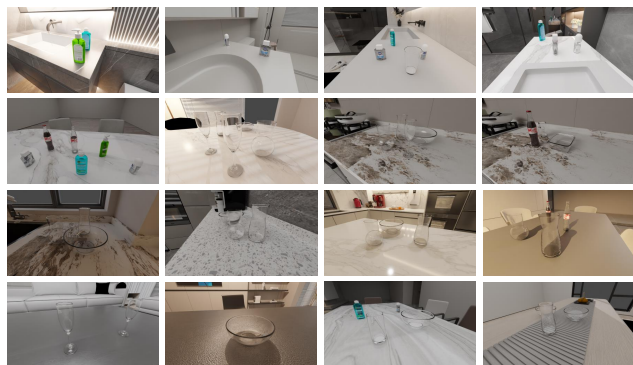


Fig. 5: Sample images from our SynClearDepth dataset are presented, showcasing randomly placed transparent objects in various indoor scenes (bathroom, dining room, kitchen, living room) under different lighting conditions. The objects include common transparent items like cosmetic packaging, glass containers, etc.

Additionally, considering the unique difficulties of transparent objects and the need for lightweight models in robotics, we designed a structural feature post-fusion architecture. Every detail of our network structure is tailored to the characteristics of transparent object scenarios.

In the comparative experiments section, the visual results demonstrate that our model significantly enhances the stereo imaging of transparent objects.

### B. Synthetic Dataset Generation



Fig. 4: The left image displays rendered models, with the first two rows featuring transparent containers such as vases, bowls, and cups, while the last two rows showcase cosmetic products made of transparent glass and plastic. The right image shows the real objects used for Sim2Real testing.

To enhance dataset generation efficiency, we utilized OptiX’s AI denoiser and deep learning super-resolution techniques [37], notably reducing the time from an average of 12.77 seconds to 4.40 seconds per set (including stereo RGB, depth, masks, and object-camera poses), significantly

speeding up the process by cutting nearly two-thirds data generation time while maintaining high-quality outputs. Our dataset generation process is illustrated in Fig. 3. Our proposed dataset SynClearDepth comprises 16 selected objects, including 10 common transparent containers in daily life and 6 products with glass material, as shown in Fig. 4. To ensure that the background of the generated dataset also contains depth value and avoid ambiguities in depth recovery training due to lack of dataset labeling of background part, we collected indoor scenes in combination with the object models, encompassing 6 bathrooms, 3 dining rooms, 5 kitchens, and 6 living rooms. Through this combination, we generated 14,091 image sets, each containing left and right RGB images with size 1280\*720, ground truth depth, instance segmentation maps, as well as object and camera poses, as illustrated in Fig. 5. In the dataset generation process, we applied domain randomization to object types, quantities, positions and poses, lighting conditions, and camera shooting angles.

### C. metrics

- 1) **AvgErr (Average Error)**: Represents the average disparity error across all pixels, indicating the general accuracy of the disparity map.
- 2) **RMS (Root Mean Square Error)**: Measures the square root of the average squared disparity error, reflecting the overall deviation from the ground truth.
- 3) **Bad 0.5 (%)**, **Bad 1.0 (%)**, **Bad 2.0 (%)**, **Bad 4.0 (%)**: These metrics indicate the percentage of pixels where the disparity error exceeds 0.5, 1.0, 2.0, and 4.0 pixels, respectively, highlighting the proportion of significant errors in the disparity map.

Together, these metrics provide a comprehensive assessment of stereo matching performance, balancing both overall accuracy and the frequency of large errors.

## IV. EXPERIMENTS

### A. Technical Specifications

Our network is firstly pre-trained on CREStereo dataset [38] and Scene Flow dataset [39], and then fine-tuned on our proposed SynClearDepth dataset for transparent object stereo imaging. Our model is trained on 1 block of NVIDIA RTX A6000 with batch size 8 and the whole training lasts for 300,000 steps. We use AdamW [40] as optimizer, the learning rate is set to 0.0002, updated with a warm-up mechanism and used one-cycle learning rate scheduler. The final learning rate when training finished is 0.0001. The input size of the model is resized to  $360 \times 720$ . Fine-tune for transparent objects takes the same training parameters as pretraining on the opaque dataset.

### B. Qualitative and Quantitative Studies for Stereo Depth Estimation

1) *Quantitative Analysis on Middlebury Dataset*: The Middlebury 2014 dataset comprises 23 pairs of images designate for training and validation purposes. We refine our model over these 23 pairs, conducting fine-tuning across 4,000 iterations with an image resolution of  $384 \times 1024$ . Benchmark against standard baseline approaches RAFT-Stereo and CREStereo using various stereo evaluation metrics further underscores the efficacy of our approach, as outlined in Tab. I. More comparison results with other methods can be found at [41].

Methods	AvgErr	RMS	bad 0.5 (%)	bad 1.0 (%)	bad 2.0 (%)	bad 4.0 (%)
RAFT-Stereo[25]	1.27	8.41	27.7	9.37	4.14	2.75
CREStereo[38]	<b>1.15</b>	<b>7.70</b>	28.0	8.25	3.71	2.04
clearDepth	1.33	8.68	<b>25.30</b>	<b>7.39</b>	<b>3.48</b>	<b>2.00</b>

TABLE I: Quantitative results on Middlebury Stereo Evaluation Benchmark [41]. All metrics have been calculated using undisclosed weighting factors. The outcomes unequivocally demonstrate that our technique significantly outperforms the baseline method.

2) *Quantitative Analysis on KITTI Dataset*: We fine-tune our pre-trained model using the KITTI 2015 training set across 5,000 steps, employing image crops sized at  $320 \times 1000$ . The learning rate is established at 0.00001, with the batch size held at 3. In terms of GRU updates, we perform 22 iterations during training, adjusting to 32 iterations for testing. Given that the labels and metrics of the KITTI dataset

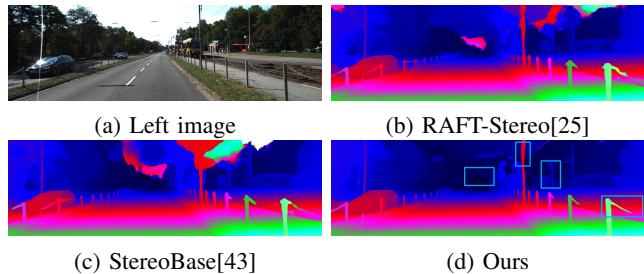


Fig. 6: Visual comparisons on KITTI 2015 with SOTA StereoBase and baseline RAFT-Stereo. Our method is more robust to overall scene details.

cannot fully reflect imaging quality [42], we conducted a qualitative analysis on the KITTI dataset. Fig. 6 demonstrates a competitive comparison focused on detail recovery, our method shows exceptional proficiency in reconstructing depth details of foreground objects, significantly outstripping alternative approaches by a substantial margin.

Methods	AvgErr	RMS	bad 0.5 (%)	bad 1.0 (%)	bad 2.0 (%)	bad 4.0 (%)
IGEV-Stereo[44]	2.0766	5.5301	58.9743	36.127	19.9668	10.7771
DLNR[45]	3.097	8.4269	28.1088	21.8442	16.481	11.9046
Selective-IGEV[46]	<b>1.273</b>	<b>4.3665</b>	34.8229	17.6288	<b>9.561</b>	5.8707
RAFT-Stereo[25]	2.245	8.8016	29.7356	17.4521	10.835	6.2107
clearDepth	2.138	8.7282	<b>24.7329</b>	<b>16.3178</b>	9.8459	<b>5.76</b>

TABLE II: Quantitative results on transparent object dataset compared with stereo SOTA methods.

3) *Evaluation on Our Transparent Object Dataset*: To validate the efficacy of our model and our proposed dataset for the task of depth recovery of transparent objects using stereo vision, we fine-tuned our pre-trained model on the SynClearDepth dataset. This fine-tuning process involved utilizing the same training parameters established during the pre-training phase. Additionally, we finetuned the baseline model, RAFT-Stereo [25] and other SOTA models on Middlebury benchmark, on the SynClearDepth dataset and conducted a performance comparison. This comparative analysis aimed to underscore the advancements and improvements our model offers in the specific context of stereo-based depth perception for transparent objects. Tab. II displays the quantitative validation results. The visualization results of the stereo imaging for transparent objects are illustrated in Fig. 7. From the visualization results, it is evident that the imaging performance of our network, specifically designed for transparent objects, significantly surpasses that of other stereo imaging methods in the transparent object regions.

4) *Ablation Study of Feature Post-Fusion Module*: To ascertain the impact of our feature post-fusion module, we embarked on a series of ablation studies. These studies compared networks equipped with and without the feature post-fusion module, specifically focusing on our transparent object dataset, SynClearDepth. The results in Tab. III demonstrate that the inclusion of the feature post-fusion module significantly improves the network's overall performance in processing transparent objects. This enhancement is particularly evident in challenging scenarios involving complex transparency and light refraction, underscoring the module's effectiveness in capturing and integrating crucial features for more accurate depth estimation and object recognition in

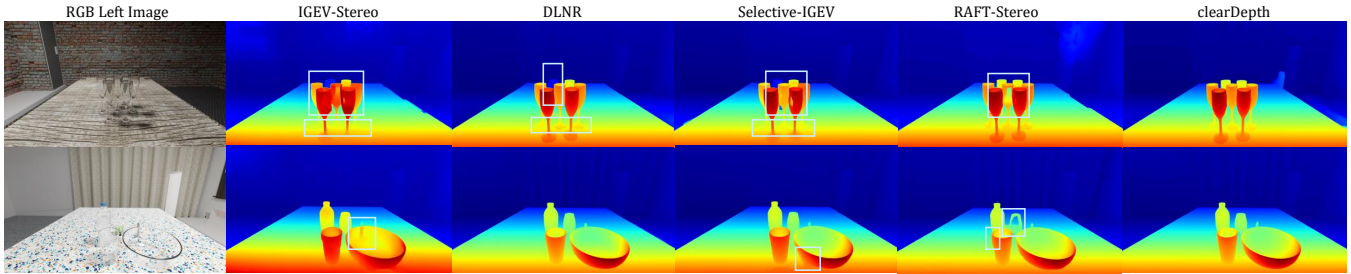


Fig. 7: The visualization results of our transparent object stereo depth reconstruction method compare with other SOTA stereo depth estimation methods by fine-tuning on SynClearDepth dataset.

such contexts. The ablation study utilizes 100,000 steps in training.

### C. Robotic Grasping Experiments

We employ the ZED 2 stereo camera with our proposed network, integrated with a robotic arm and a five-fingered dexterous hand, to perform grasping tasks. We tested the success rate of grasping transparent objects in service robot scenarios, following the experimental setup of FFHCluttered-Grasping [47]. Using our stereo method, we generated point clouds of scenes with transparent objects and performed pose estimation. We then planned the grasping posture for the five-fingered hand. We conducted 150 experiments for each scenario, varying the number of transparent objects from 1 to 5, and the results are shown in Table IV. We achieved an average success rate of 86.2%. Our approach integrates seamlessly into existing robotic grasping frameworks without needing additional processing of intermediate results. Our method does not require multi-view images capture, thus maintaining the robot’s operational efficiency. Additionally, our data generation process is fast and efficient, enabling rapid expansion of datasets for further tasks. Our findings demonstrate that our transparent object depth recovery network significantly improves the robot’s ability to grasp transparent objects.

Methods	AvgErr	RMS	bad 0.5 (%)	bad 1.0 (%)	bad 2.0 (%)	bad 4.0 (%)
w/o Fusion	6.90	15.48	43.34	29.63	21.52	16.62
Feature Fusion	<b>2.64</b>	<b>8.59</b>	<b>27.23</b>	<b>16.87</b>	<b>11.28</b>	<b>7.72</b>

TABLE III: Ablation study for the feature post-fusion module in clearDepth with 100,000 steps on SynClearDepth dataset.

Object Number	1	2	3	4	5
success rate	98%	92%	86%	78%	76%

TABLE IV: Grasping success rate with varying number of transparent objects.

## V. CONCLUSION

In this paper, we propose a new stereo transparent object dataset SynClearDepth, containing RGB, depth, mask, object poses, and camera poses. Compared to other real datasets, our simulated data does not introduce the inherent noise of real 3D sensors. Unlike other simulated datasets, we have collected a large number of indoor scene models to

fill the dataset background, avoiding ambiguities for depth recovery networks. We also propose a stereo depth recovery network for transparent objects, which enhances the underlying structural information, allowing our network to recover the depth of transparent objects implicitly without the need for a transparent object mask prior. We conducted comprehensive comparative experiments on our model using both public datasets and our proprietary dataset for transparent objects. Additionally, we performed ablation studies to evaluate the design of our model. These experiments demonstrated the exceptional performance of our model, highlighting its robustness and accuracy in various scenarios for transparent object perception, aiding in the manipulation tasks of transparent objects by robots.

## REFERENCES

- [1] J. Jiang, G. Cao, J. Deng, T.-T. Do, and S. Luo, “Robotic perception of transparent objects: A review,” *IEEE Transactions on Artificial Intelligence*, 2023.
- [2] T. Li, Z. Chen, H. Liu, and C. Wang, “FdcT: Fast depth completion for transparent objects,” *IEEE Robotics and Automation Letters*, 2023.
- [3] K. Chen, S. Wang, B. Xia, D. Li, Z. Kan, and B. Li, “Tode-trans: Transparent object depth estimation with transformer,” in *2023 IEEE International Conference on Robotics and Automation (ICRA)*. IEEE, 2023, pp. 4880–4886.
- [4] K. Chen, S. James, C. Sui, Y.-H. Liu, P. Abbeel, and Q. Dou, “StereoPose: Category-level 6d transparent object pose estimation from stereo images via back-view nocs,” in *2023 IEEE International Conference on Robotics and Automation (ICRA)*. IEEE, 2023, pp. 2855–2861.
- [5] Y. R. Wang, Y. Zhao, H. Xu, S. Eppel, A. Aspuru-Guzik, F. Shkurti, and A. Garg, “Mvtrans: Multi-view perception of transparent objects,” in *2023 IEEE International Conference on Robotics and Automation (ICRA)*. IEEE, 2023, pp. 3771–3778.
- [6] Y. Cao, Z. Zhang, E. Xie, Q. Hou, K. Zhao, X. Luo, and J. Tuo, “Fakemix augmentation improves transparent object detection,” *arXiv preprint arXiv:2103.13279*, 2021.
- [7] M. Shao, C. Xia, D. Duan, and X. Wang, “Polarimetric inverse rendering for transparent shapes reconstruction,” *arXiv preprint arXiv:2208.11836*, 2022.
- [8] H. Fang, H.-S. Fang, S. Xu, and C. Lu, “Transcg: A large-scale real-world dataset for transparent object depth completion and a grasping baseline,” *IEEE Robotics and Automation Letters*, vol. 7, no. 3, pp. 7383–7390, 2022.
- [9] H. Xu, Y. R. Wang, S. Eppel, A. Aspuru-Guzik, F. Shkurti, and A. Garg, “Seeing glass: joint point cloud and depth completion for transparent objects,” *arXiv preprint arXiv:2110.00087*, 2021.
- [10] S. Sajjan, M. Moore, M. Pan, G. Nagaraja, J. Lee, A. Zeng, and S. Song, “Clear grasp: 3d shape estimation of transparent objects for manipulation,” in *2020 IEEE International Conference on Robotics and Automation (ICRA)*. IEEE, 2020, pp. 3634–3642.
- [11] X. Chen, H. Zhang, Z. Yu, A. Opipari, and O. Chadwicke Jenkins, “Clearpose: Large-scale transparent object dataset and benchmark,” in *European Conference on Computer Vision*. Springer, 2022, pp. 381–396.

- [12] A. Kalra, V. Taamazyan, S. K. Rao, K. Venkataraman, R. Raskar, and A. Kadambi, "Deep polarization cues for transparent object segmentation," in *Proceedings of the IEEE/CVF Conference on Computer Vision and Pattern Recognition*, 2020, pp. 8602–8611.
- [13] K. Garigapati, E. Blasch, J. Wei, and H. Ling, "Transparent object tracking with enhanced fusion module," in *2023 IEEE/RSJ International Conference on Intelligent Robots and Systems (IROS)*. IEEE, 2023, pp. 7696–7703.
- [14] A. Lukezic, Z. Trojer, J. Matas, and M. Kristan, "Trans2k: Unlocking the power of deep models for transparent object tracking," *arXiv preprint arXiv:2210.03436*, 2022.
- [15] H. Cai, F. Xue, L. Xu, and L. Guo, "Transmatting: Tri-token equipped transformer model for image matting," *arXiv preprint arXiv:2303.06476*, 2023.
- [16] Q. Dai, J. Zhang, Q. Li, T. Wu, H. Dong, Z. Liu, P. Tan, and H. Wang, "Domain randomization-enhanced depth simulation and restoration for perceiving and grasping specular and transparent objects," in *European Conference on Computer Vision*. Springer, 2022, pp. 374–391.
- [17] Z. Li, X. Long, Y. Wang, T. Cao, W. Wang, F. Luo, and C. Xiao, "Neto: Neural reconstruction of transparent objects with self-occlusion aware refraction-tracing," *arXiv preprint arXiv:2303.11219*, 2023.
- [18] Q. Dai, Y. Zhu, Y. Geng, C. Ruan, J. Zhang, and H. Wang, "Grasprnf: Multiview-based 6-dof grasp detection for transparent and specular objects using generalizable nerf," in *2023 IEEE International Conference on Robotics and Automation (ICRA)*. IEEE, 2023, pp. 1757–1763.
- [19] Z. Li, Y.-Y. Yeh, and M. Chandraker, "Through the looking glass: neural 3d reconstruction of transparent shapes," in *Proceedings of the IEEE/CVF Conference on Computer Vision and Pattern Recognition*, 2020, pp. 1262–1271.
- [20] H. Zhang, A. Opipari, X. Chen, J. Zhu, Z. Yu, and O. C. Jenkins, "Transnet: Transparent object manipulation through category-level pose estimation," *arXiv preprint arXiv:2307.12400*, 2023.
- [21] N. Mayer, E. Ilg, P. Häusser, P. Fischer, D. Cremers, A. Dosovitskiy, and T. Brox, "A large dataset to train convolutional networks for disparity, optical flow, and scene flow estimation," in *Proceedings of the IEEE conference on computer vision and pattern recognition*, 2016, pp. 4040–4048.
- [22] H. Xu and J. Zhang, "Aanet: Adaptive aggregation network for efficient stereo matching," in *Proceedings of the IEEE/CVF Conference on Computer Vision and Pattern Recognition*, 2020, pp. 1959–1968.
- [23] Y. Cao, J. Xu, S. Lin, F. Wei, and H. Hu, "Gcnet: Non-local networks meet squeeze-excitation networks and beyond," in *Proceedings of the IEEE/CVF international conference on computer vision workshops*, 2019, pp. 0–0.
- [24] J.-R. Chang and Y.-S. Chen, "Pyramid stereo matching network," in *Proceedings of the IEEE conference on computer vision and pattern recognition*, 2018, pp. 5410–5418.
- [25] L. Lipson, Z. Teed, and J. Deng, "Raft-stereo: Multilevel recurrent field transforms for stereo matching," in *2021 International Conference on 3D Vision (3DV)*. IEEE, 2021, pp. 218–227.
- [26] Z. Teed and J. Deng, "Raft: Recurrent all-pairs field transforms for optical flow," in *Computer Vision—ECCV 2020: 16th European Conference, Glasgow, UK, August 23–28, 2020, Proceedings, Part II 16*. Springer, 2020, pp. 402–419.
- [27] Z. Li, X. Liu, N. Drenkow, A. Ding, F. X. Creighton, R. H. Taylor, and M. Unberath, "Revisiting stereo depth estimation from a sequence-to-sequence perspective with transformers," in *Proceedings of the IEEE/CVF international conference on computer vision*, 2021, pp. 6197–6206.
- [28] P.-E. Sarlin, D. DeTone, T. Malisiewicz, and A. Rabinovich, "SuperGlue: Learning feature matching with graph neural networks," in *Proceedings of the IEEE/CVF conference on computer vision and pattern recognition*, 2020, pp. 4938–4947.
- [29] J. Kim, M.-H. Jeon, S. Jung, W. Yang, M. Jung, J. Shin, and A. Kim, "Transpose: Large-scale multispectral dataset for transparent object," *The International Journal of Robotics Research*, p. 02783649231213117, 2024.
- [30] J. Jiang, G. Cao, T.-T. Do, and S. Luo, "A4t: Hierarchical affordance detection for transparent objects depth reconstruction and manipulation," *IEEE Robotics and Automation Letters*, vol. 7, no. 4, pp. 9826–9833, 2022.
- [31] L. Zhu, A. Mousavian, Y. Xiang, H. Mazhar, J. van Eenbergen, S. Debnath, and D. Fox, "Rgb-d local implicit function for depth completion of transparent objects," in *Proceedings of the IEEE/CVF Conference on Computer Vision and Pattern Recognition*, 2021, pp. 4649–4658.
- [32] J. Ichnowski, Y. Avigal, J. Kerr, and K. Goldberg, "Dex-nerf: Using a neural radiance field to grasp transparent objects," *arXiv preprint arXiv:2110.14217*, 2021.
- [33] J. Shi, Y. Jin, D. Li, H. Niu, Z. Jin, H. Wang *et al.*, "Asgrasp: Generalizable transparent object reconstruction and grasping from rgb-d active stereo camera," *arXiv preprint arXiv:2405.05648*, 2024.
- [34] S. Tuli, I. Dasgupta, E. Grant, and T. L. Griffiths, "Are convolutional neural networks or transformers more like human vision?" *arXiv preprint arXiv:2105.07197*, 2021.
- [35] E. Xie, W. Wang, Z. Yu, A. Anandkumar, J. M. Alvarez, and P. Luo, "Segformer: Simple and efficient design for semantic segmentation with transformers," *Advances in Neural Information Processing Systems*, vol. 34, pp. 12 077–12 090, 2021.
- [36] M. Oquab, T. Darcet, T. Moutakanni, H. Vo, M. Szafraniec, V. Khali-dov, P. Fernandez, D. Haziza, F. Massa, A. El-Nouby *et al.*, "Dinov2: Learning robust visual features without supervision," *arXiv preprint arXiv:2304.07193*, 2023.
- [37] N. Ahn, B. Kang, and K.-A. Sohn, "Fast, accurate, and lightweight super-resolution with cascading residual network," in *Proceedings of the European conference on computer vision (ECCV)*, 2018, pp. 252–268.
- [38] J. Li, P. Wang, P. Xiong, T. Cai, Z. Yan, L. Yang, J. Liu, H. Fan, and S. Liu, "Practical stereo matching via cascaded recurrent network with adaptive correlation," in *Proceedings of the IEEE/CVF conference on computer vision and pattern recognition*, 2022, pp. 16 263–16 272.
- [39] N. Mayer, E. Ilg, P. Häusser, P. Fischer, D. Cremers, A. Dosovitskiy, and T. Brox, "A large dataset to train convolutional networks for disparity, optical flow, and scene flow estimation," in *IEEE International Conference on Computer Vision and Pattern Recognition (CVPR)*, 2016, arXiv:1512.02134. [Online]. Available: <http://lmb.informatik.uni-freiburg.de/Publications/2016/MIFDB16>
- [40] I. Loshchilov and F. Hutter, "Decoupled weight decay regularization," 2019.
- [41] "Middlebury stereo vision page," <https://vision.middlebury.edu/stereo/>.
- [42] L. Yang, B. Kang, Z. Huang, Z. Zhao, X. Xu, J. Feng, and H. Zhao, "Depth anything v2," *arXiv:2406.09414*, 2024.
- [43] X. Guo, J. Lu, C. Zhang, Y. Wang, Y. Duan, T. Yang, Z. Zhu, and L. Chen, "Openstereo: A comprehensive benchmark for stereo matching and strong baseline," 2023.
- [44] G. Xu, X. Wang, X. Ding, and X. Yang, "Iterative geometry encoding volume for stereo matching," in *Proceedings of the IEEE/CVF Conference on Computer Vision and Pattern Recognition*, 2023, pp. 21 919–21 928.
- [45] H. Zhao, H. Zhou, Y. Zhang, J. Chen, Y. Yang, and Y. Zhao, "High-frequency stereo matching network," in *Proceedings of the IEEE/CVF Conference on Computer Vision and Pattern Recognition*, 2023, pp. 1327–1336.
- [46] X. Wang, G. Xu, H. Jia, and X. Yang, "Selective-stereo: Adaptive frequency information selection for stereo matching," in *Proceedings of the IEEE/CVF Conference on Computer Vision and Pattern Recognition*, 2024, pp. 19 701–19 710.
- [47] L. Zhang, K. Bai, G. Huang, Z. Chen, and J. Zhang, "Multi-fingered robotic hand grasping in cluttered environments through hand-object contact semantic mapping," *arXiv preprint arXiv:2404.08844*, 2024.